A Method of Accurate Position Control with a Pneumatic Cylinder Driving Apparatus

Ji-Seong Jang*
Division of Mechanical Engineering, Pukyong National University, San 100, Yongdang-Dong, Nam-Gu, Busan 608-739, Korea
Jung-Hoan Byun
Faculty of Marine Technology, Chonnam National University, San 96-1, Dundeok-Dong, Yeosu, Jeollanam-Do 550-749, Korea

In this paper, a method of accurate position control using a pneumatic cylinder driving apparatus is presented. To overcome the effect of friction force and transmission line, low friction type cylinder applied externally pressurized air bearing structure is used and two control valves attached both side of the cylinder directly. To compensate nonlinear characteristics of control valves, linearized control input derived from the relation between control input and effective area of control valve, and dither signal are applied to the valve. The controller applied to the pneumatic cylinder driving apparatus is composed of a state feedback controller and a disturbance observer. Experimental results show that the effectiveness of the proposed method and position control error of 5 μm accuracy could be obtained easily.

Key Words : Accurate Position Control, Nonlinear Characteristics, Pneumatic Cylinder Driving Apparatus

1. Introduction

Pneumatic cylinder driving apparatus are widely used in industrial applications owing to the easy installation and maintenance. However, the most common application of the pneumatic cylinder driving apparatus is a simply repeating operation (Johira, 1997 ; McGuirk et al., 1998) because it is not easy to obtain high performance position control results due to several nonlinear characteristics such as compressibility of air, friction force of cylinder and nonlinear characteristics of control valve (Kawai et al., 1993 ; Tokashiki et al., 2000 ; Yoshimitu et al, 2002). Therefore studies on position control with pneumatic cylinder driving apparatus have concentrated on the compensation of nonlinearities mentioned above. In the previous studies, methods to improve position control accuracy of pneumatic driving apparatus divide into two categories. The one is to compensate nonlinear characteristics with a high level controller such as nonlinear controller, adaptive controller, H_∞ controller and switching controller etc. (Kimura et al., 2003 ; Lai et al., 1990 ; Situm et al., 2004). The other is to decrease the effect of friction force using an additional equipment (Kawashima et al., 1998 ; Saito et al., 1995). As mentioned above, various methods were applied to improve position control accuracy of pneumatic cylinder driving apparatus, but, position control accuracy using only a high level controller are limited and the controllers realized position control errors about 1 [mm]~0.2 [mm], and, the methods using an additional equipment did not consider and compensate the nonlinear characteristics except friction force.

* Corresponding Author,
E-mail : jangjs@pknu.ac.kr
TEL : +82-51-620-1583; **FAX** : +82-51-620-1574
Division of Mechanical Engineering, Pukyong National University, San 100, Yongdang-Dong, Nam-Gu, Busan 608-739, Korea. (Manuscript **Received** November 17, 2005; **Revised** April 6, 2006)

In this study, a method of accurate position control using a pneumatic cylinder driving apparatus is proposed. The piston of cylinder used in the pneumatic cylinder driving apparatus is mounted with externally pressurized air bearing to compensate friction force on the piston, and, control valves are connected both side of the cylinder directly to reduce the influence of transmission line. To compensate the nonlinear characteristics of the control valve, linearized control input derived from the relation between control input and effective area of control valve and dither signal are used. The controller applied to the pneumatic cylinder driving apparatus is composed of a state feedback controller which feeds back position, velocity and pressure, and a disturbance observer to reduce the effect of model discrepancy and compressibility of air cause by the change of operating points. The performance of the proposed method is evaluated by experiments and the experimental results show that position control accuracy of pneumatic cylinder driving apparatus is improved remarkably and position control error of 5 μm accuracy could be obtained easily.

2. Configuration of the Driving Apparatus

Figure 1 shows the configuration of the driving apparatus. It is primarily composed of a pneumatic cylinder, two control valves, two pressure transducers and a displacement transducer.

The pneumatic cylinder is rod-less type whose length is 200 [mm], width is 100 [mm], height is 50 [mm] and the stroke is 50 [mm]. Figure 2 shows the structure of the cylinder. Figure 2(a) is photograph of the cylinder, (b) and (c) are sectional drawings shown by the arrows marked on (a). Piston is mounted with externally pressurized air bearing and seal used on normal pneumatic cylinder is eliminated. The shape of driving piston is a box type and it is inserted into the cylinder body which has a hole on the upper part. There are four chambers, $V_1 \sim V_4$, between cylinder body

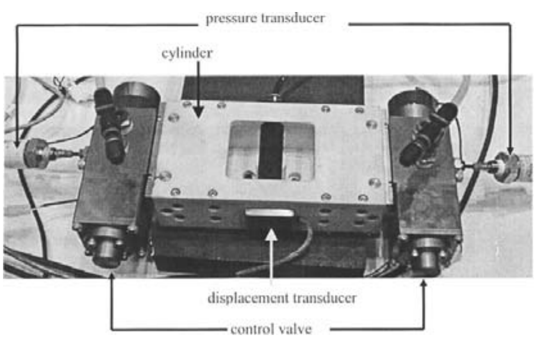

Fig. 1 Configuration of the pneumatic cylinder driving apparatus

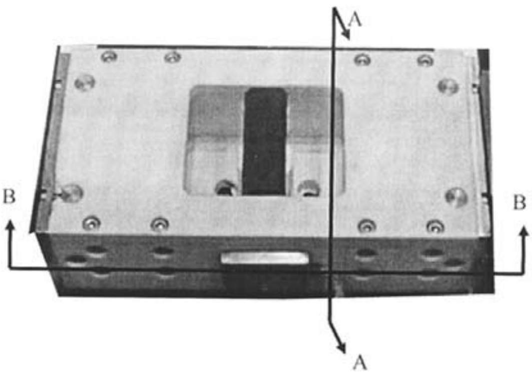

(a) Photograph of the cylinder

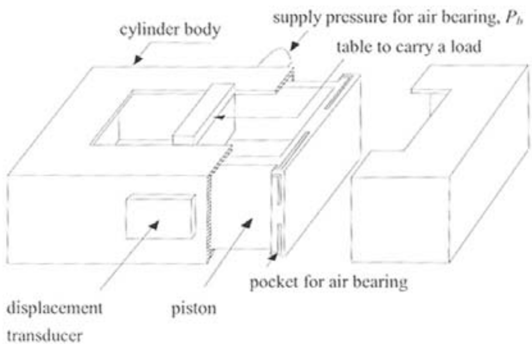

(b) A-A sectional drawing

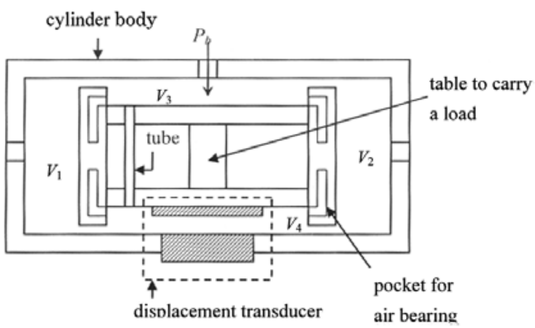

(c) B-B sectional drawing

Fig. 2 Structure of the cylinder

and piston. The chambers do not connect with the upper hole of cylinder body wherever the piston moves and V_3 connected with V_4 through a tube to match the pressure in V_3 with V_4. Pockets for air bearing are installed on the surface of the piston. When supply pressure for air bearing, P_b, is supplied, the air flows into the pockets from V_3 and V_4, and, the air flows into V_1, V_2 from the pockets. Therefore, piston does not contact with the cylinder body because of the operation of air bearing, and, displacement of the piston can be controlled without affecting friction force.

Figure 3 shows measurement results of friction force on the piston. In a general measurement method (Helduser et al., 1998), it is difficult to measure the friction force because full stroke of the cylinder is short. Therefore, friction forced is estimated by using the difference between inertia force and driving force of piston. In Fig. 3, x, v and a represent displacement, velocity and acceleration of the piston respectively, F is inertia force calculated from acceleration of the piston (dot dashed line) or driving force translated from pressure difference in V_1 and V_2 (solid line), A is the pressurized area of the piston, M is the driving mass and F_r is the friction force on the piston, and, Fig. 3(a) ~ (c) are in case that initial positions of the piston are set to 25 [mm], 10 [mm] and 40 [mm] respectively. These results show that friction force on the piston is below than 0.5 [N] at all velocity range and at all position. Static friction force on labyrinth seal type pneumatic cylinder, which has been known that friction force is smaller than normal o-ring seal type pneumatic cylinder, is about 10 [N] (Kosaki et al., 2002). Therefore, we know that friction force on the cylinder is much smaller than normal pneumatic cylinder.

The control valves (Kolvenbach KG, EWS3/6) used in the driving apparatus are 3 port type servo valves. Figure 4 shows the nonlinear characteristics between control input u [V] and effective area S_e [mm^2] of the control valve.

The position measurement is carried out by a digital counter (Mitsutoyo, ST211, resolution 1 μm) and the pressure in the cylinder chamber is

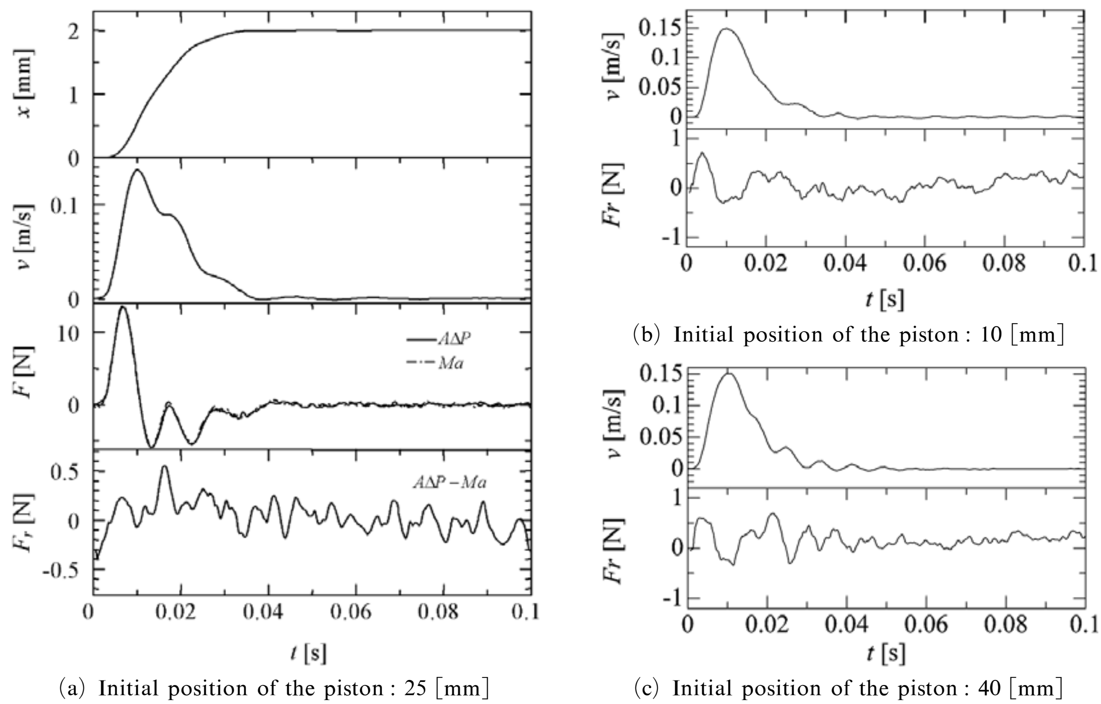

(a) Initial position of the piston : 25 [mm]

(b) Initial position of the piston : 10 [mm]

(c) Initial position of the piston : 40 [mm]

Fig. 3 Estimation results of friction force on the cylinder according to the change of initial position of the piston

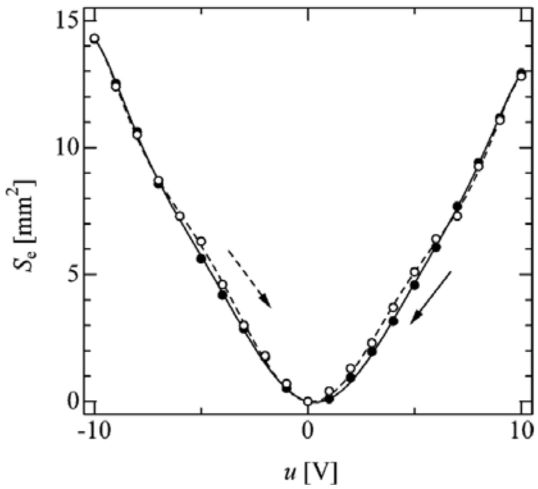

Fig. 4 Measured results of nonlinear characteristics of the control valve

measured by pressure transducer (Toyoda, SD200, resolution 0.3 kPa)

3. Modeling

Figure 5 shows the schematic representation of the pneumatic cylinder driving apparatus.

In Fig. 5, G [kg/s] is the mass flow rate, L [m] is the cylinder full stroke, M [kg] is the driving mass, P [Pa] is the absolute pressure, T [K] is the absolute temperature, V [m^3] is the control volume, x [m] is the displacement, and subscript 1, 2 mean the incoming side and the outgoing side respectively, and subscript a, b mean the supply and the atmosphere respectively.

Eqs. (1) and (2) describe the dynamic pressure change in the control volumes. Here it is assumed that air is a perfect gas, pressure and temperature within the control volumes are homogeneous and the process is adiabatic.

$$\frac{dP_1}{dt}=\frac{\kappa}{V_1}\left\{-P_1A\frac{dx}{dt}+G_1RT_1\right\} \tag{1}$$

$$\frac{dP_2}{dt}=\frac{\kappa}{V_2}\left\{P_2A\frac{dx}{dt}+G_2RT_2\right\} \tag{2}$$

In Eqs. (1) and (2), κ is the specific heat ratio, A [m^2] is the pressurized area of the piston and R [J/(kg·K)] is the gas constant. Eq. (3) shows

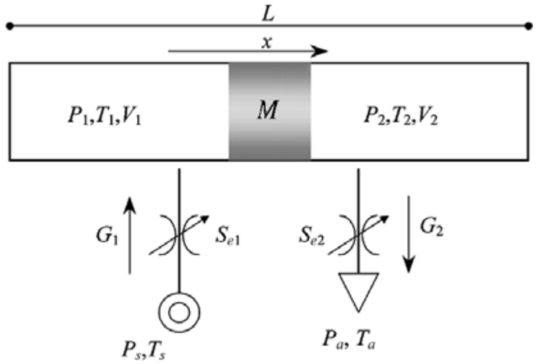

Fig. 5 Schematic diagram of the driving apparatus

Table 1 Physical parameters of the driving apparatus

A [m^2]	$2.7\cdot10^{-3}$	R [J/(kgK)]	287
k_q [(kg/s)/V]	$4.17\cdot10^{-4}$	T_a [K]	293
L [m]	0.05	x_0 [m]	0.025
M [kg]	0.48	κ	1.4
P_0[Pa]	$1.4\cdot10^5$		

dynamic equation.

$$\begin{aligned} M\frac{d^2x}{dt^2}&=A(P_1-P_2)-F_r,\\ &=B\frac{dx}{dt}+F_c\,\mathrm{sgn}\left(\frac{dx}{dt}\right) \end{aligned} \tag{3}$$

In Eq. (3), B [N/(m/s)] is the dynamic friction coefficient, F_c [N] is the static friction force.

At an operating point $G_1=-G_2=G_0=k_q\cdot u$, $x=x_0$, $P_1=P_2=P_0$, $V_1=V_2=V_0$, and $T_1=T_2=T_a$, Eqs. (1) ~ (3) can be expressed as follows.

$$\frac{d}{dt}\begin{bmatrix}x\\v\\P_1\\P_2\end{bmatrix}=\begin{bmatrix}0&1&0&0\\0&0&\frac{A}{M}&-\frac{A}{M}\\0&-\frac{\kappa P_0}{x_0}&0&0\\0&\frac{\kappa P_0}{L-x_0}&0&0\end{bmatrix}\begin{bmatrix}x\\v\\P_1\\P_2\end{bmatrix}+\begin{bmatrix}0\\0\\\frac{\kappa k_qRT_a}{Ax_0}\\-\frac{\kappa k_qRT_a}{A(L-x_0)}\end{bmatrix}u, \tag{4}$$

$$x=[1\ 0\ 0\ 0][x\ v\ P_1\ P_2]^T$$

In Eq. (4), v [m/s] is the velocity of the piston, k_q [(kg/s)/V] is the flow gain of the control valve, and it is assumed that friction force F_r on the piston is negligible. Table 1 shows physical parameters of the driving apparatus.

4. Controller Design

4.1 State feedback controller design

From the Eq. (4), the relationship between control input, $u(s)$, and displacement of the piston, $x(s)$, can be represented by

$$\frac{x(s)}{u(s)}=\frac{\kappa_n\omega_n^2}{s(s^2+\omega_n^2)}=H(s), \quad k_n=\frac{k_qRT_a}{AP_0},\ \omega_n^2=\frac{\kappa AP_0L}{Mx_0(L-x_0)} \tag{5}$$

As it can be seen in Eq. (5), damping characteristics of the driving apparatus becomes more serious because the operation of air bearing. In this case, minor-loop compensation using velocity and acceleration of the piston can be applied to improve the damping effect and dynamic performance. Considering the minor-loop compensation, output from controller becomes

$$u=K_p(x_r-x)-K_vv-K_aa \tag{6}$$

where x_r is the reference position, K_p [V/m] is the proportional gain, K_v [V/(m/s)] is the velocity gain and K_a[V/(m/s^2)] is the acceleration gain. Velocity and acceleration in Eq. (6) can be obtained by differentiation of position, but, phase delay is occurred when approximated differentiation is used to get velocity and acceleration from position, and phase delay of acceleration is more serious than it of velocity. Therefore, acceleration of the piston is calculated using the mass of the driving part, pressurized area of the piston and pressure difference between P_1 and P_2. Figure 6 shows block diagram of control system with the state feedback controller.

In Fig. 6, closed loop transfer function from x_r to x becomes

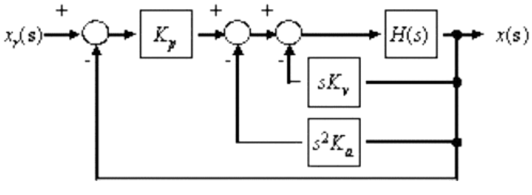

Fig. 6 Block diagram of the control system with the state feedback controller

$$\frac{x(s)}{x_r(s)}=\frac{k_n\omega_n^2K_p}{s^3+k_n\omega_n^2K_as^2+(k_n\omega_n^2K_v+\omega_n^2)s+k_n\omega_n^2K_p}=H_m(s) \tag{7}$$

In case that K_p is selected to be a value, control gains of the state feedback controller can be regulated as follows (Jang, 2002).

$$K_v=[\beta(k_n\omega_n^2K_p)^{2/3}-\omega_n^2]/k_n\omega_n^2, \quad K_a=[\alpha(k_n\omega_n^2K_p)^{1/3}]/k_n\omega_n^2 \tag{8}$$

where α and β are dimensionless parameters to adjust phase margin and gain margin of the control system (Hanafusa, 1982). In order to specify the phase margin is 77 [deg] and gain margin is 16[dB], α and β are set to be 2 and 3 respectively. In this study, K_p is selected to be 7000, therefore K_v and K_a using Eq. (8) are given by 43.7 and 0.094 respectively.

4.2 Compensation of nonlinear characteristics of control valve

In Fig. 4, it can be known that two nonlinear characteristics are presented between control input and effective area of control valve. The one is the nonlinearity of $\Delta S_e/\Delta u$ described in ① of Fig. 7(a) and the other is the hysteresis characteristics described in ③ of Fig. 7(b). In Fig. 7(b) x_{spl} means displacement of spool of control valve. To compensate the nonlinearity described in ① of Fig. 7(a), linearized control input $\hat{u}$ derived from the relation between S_e and u is applied to the control valve in place of u, therefore, in appearance, control valve has a linearized control input-effective area characteristics described in ② of Fig. 7 (a). Eq. (9) shows the relation between $\hat{u}$ and u.

$$\begin{aligned}&\text{if } u\geq 0.0,\ \hat{u}=f_1(u),\\ &f_1(u)=0.06408+3.02974\cdot u-0.92668\cdot u^2\\ &\qquad+0.18463\cdot u^3-0.01729\cdot u^4+0.000606\cdot u^5\\ &\text{if } u<0.0,\ \hat{u}=f_2(u),\\ &f_2(u)=0.01313+1.87095\cdot u+0.35396\cdot u^2\\ &\qquad+0.06559\cdot u^3+0.00609\cdot u^4+0.000213\cdot u^5\end{aligned} \tag{9}$$

To reduce the hysteresis, a dither signal, frequency is 250 [Hz] and magnitude is ±0.3 [V], is

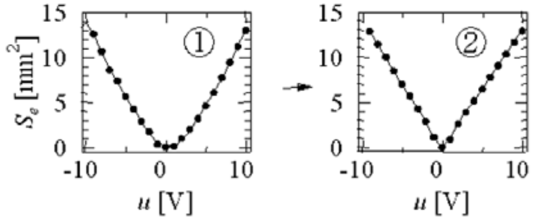

(a) Input-output characteristics

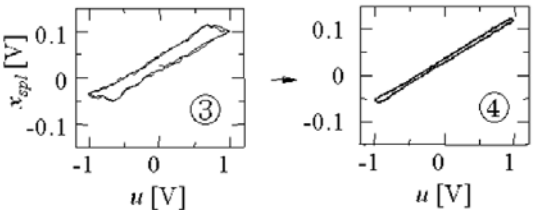

(b) Hysteresis characteristics

Fig. 7 Compensated results of nonlinear characteristics of control valve using linearized input and dither signal

inputted to the control valve. ④ of Fig. 7(b) shows that hysteresis is reduced remarkably by using the dither signal.

4.3 Disturbance observer design

To compensate the nonlinear characteristics of the driving apparatus, such as compressibility of air, and variation of natural frequency according to the change of operating position of the piston, pressure and temperature in the control volume, disturbance observer is designed. Fig. 8 shows block diagram of the control system with disturbance observer.

In Fig. 8, $H_n(s)$ is the position control system including state feedback controller, $H_m(s)$ is the nominal model described in Eq. (7), $d(s)$ is a disturbance representing modeling error of $H_n(s)$, $Q(s)$ is a stabilizing filter and e^{-Ls} is the time delay of the driving apparatus. Closed loop transfer function form $x_r(s)$ and $d(s)$ to $x(s)$, and sensitivity transfer function, $S(s)$, using the disturbance observer are given by

$$x(s)=\frac{e^{-Ls}(x_r(s)-(1-e^{-Ls}(s)a(s))d(s))}{H_m^{-1}(s)Q(s)+H_n^{-1}(s)(1-Q(s))} \tag{10}$$
$$S(s)=1-e^{-Ls}Q(s)$$

From Eq. (10), if $\|Q(s)\|$ approaches 1 then

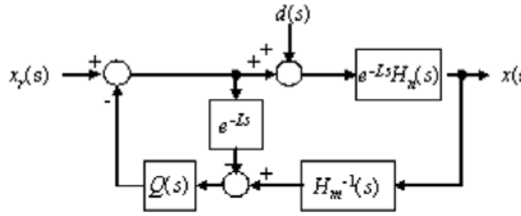

Fig. 8 Block diagram of the control system with the disturbance observer

$x(s)/x_r(s)=e^{-Ls}H_m(s)$ and $\|S(s)\|$ gradually reduced, therefore, it can be known that the disturbance observer estimate and compensate the modeling error within a frequency band of $\|Q(s)\|=1$. Delay time e^{-Ls} in Eq. (10) is assumed to be 4 [ms] using the results described in Fig. 3(a). Stabilizing filter $Q(s)$ is constructed from a reduced order observer having multiple poles. Designed $Q(s)$ is as follows.

$$Q(s)=w^3/(s+w)^3,\ w=1000 \tag{11}$$

In Eq. (11), w is selected to be $\|S(s)\|$ becomes smaller than $\|1-e^{-Ls}H_m(s)\|$ within the frequency band of $\|Q(s)\|=1$.

5. Experimental Results and Discussions

Figure 9 shows the position control results in case that characteristics of the control valve is changed according to the combination of the nonlinear characteristics described in Fig. 7. In Fig. 9, initial position of the piston, x_0, is set to be 25 [mm]. In Fig. 9, it can be observed that the result using the combination of ② and ④, control input-effective area characteristics is linearized and the dither is used, shows higher dynamic response and smaller position control error than the other cases.

Figures 10～12 show position control results with the proposed method. To confirm the repeated position control performance, experiments are performed 30 times repeatedly. Figure 10 shows the examples of the position control results in case of the change of the initial position of the piston.

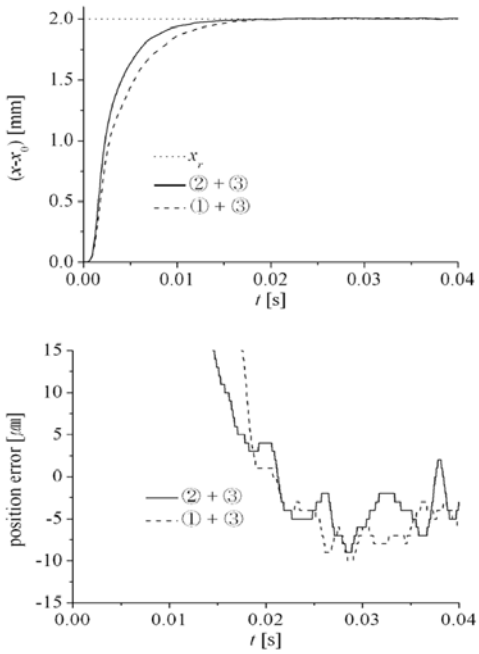

(a) Effect of the input-output characteristics of control valve on the position control accuracy

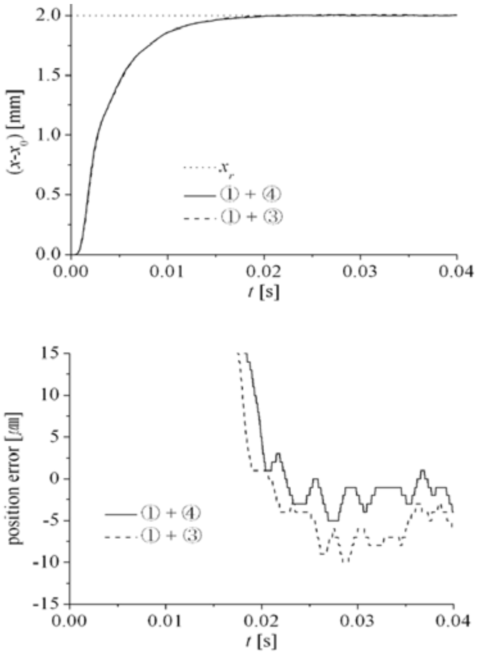

(b) Effect of the hysteresis characteristics of the control valve on the position control accuracy

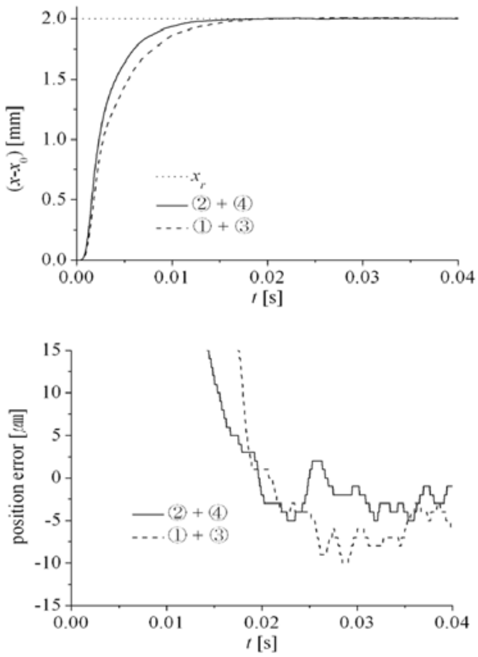

(c) Mixed effect of the input-output characteristics and the hysteresis characteristics of the control valve on the position control accuracy

Fig. 9 Effect of the nonlinear characteristics of the control valve described in Fig. 7 on the position control accuracy (initial position of the piston : 25 [mm])

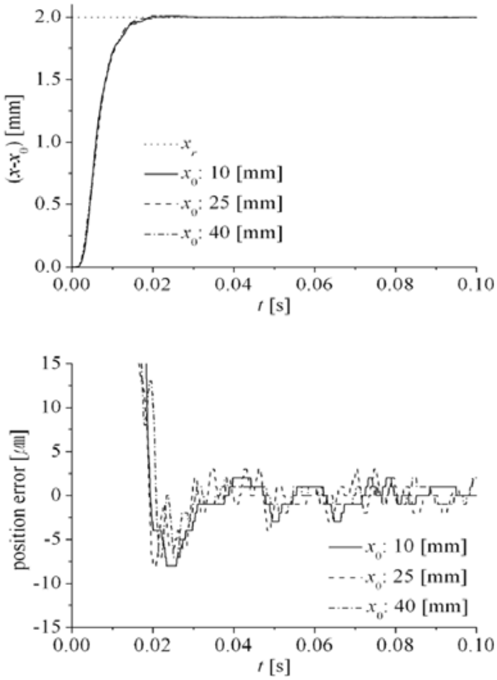

Fig. 10 Position control results in case of the change of the initial position of the piston

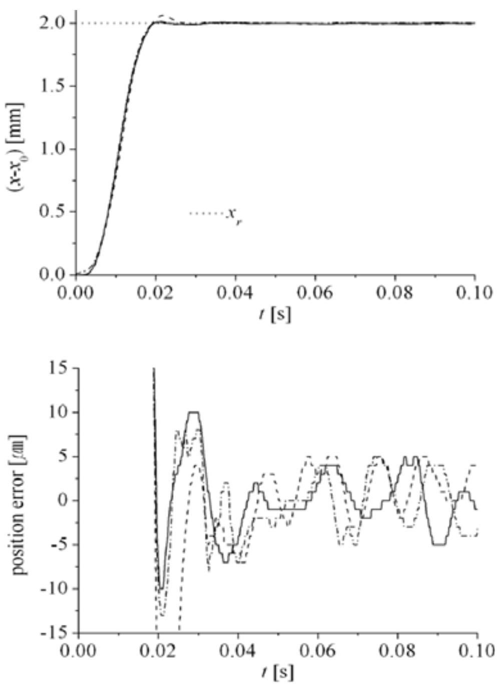

Fig. 11 Examples for repeated position control results (initial position of the piston : 25 [mm], step width : 2 [mm])

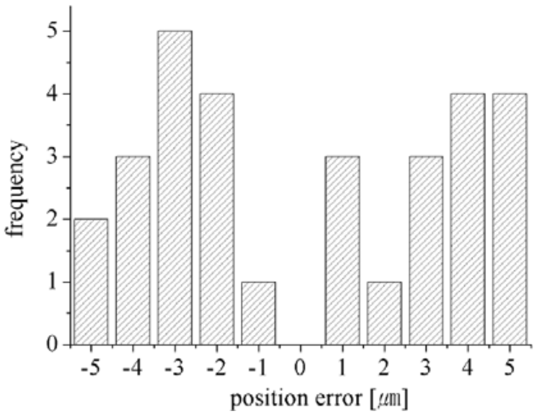

Fig. 12 The result of investigating position control errors (initial position of the piston : 25 [mm], step width : 2 [mm])

In Fig. 10, it is clear that transient response of the piston with the controller is not changed by the variation of initial position and, position control errors remain within ± 5 [μm]. Figure 11 shows the examples of the position control results when initial position and step width of the piston are set to be 25 [mm] and 2 [mm] respectively.

In Fig. 11, it can be known that position control errors remain within ± 5 [μm] after 0.045 [s].

Figure 12 shows the result of investigating position control errors when initial position and step width of the piston are set to be 25 [mm] and 2 [mm] respectively.

In Fig. 12, position control errors express the errors on 0.045 [s], and the mean value and standard deviation of the errors are 0.133 [μm] and 3.6 [μm] respectively.

6. Conclusions

It has been known that accurate position control with a pneumatic cylinder driving apparatus is not easy because of several nonlinear characteristics such as compressibility of air, friction force of cylinder and nonlinear characteristics of control valve.

In this paper, a method of accurate position control using a pneumatic cylinder driving apparatus is presented. To overcome the friction force, low friction type cylinder applied externally pressurized air bearing structure is used, and, two control valves attached both side of the cylinder directly to eliminate the effect of transmission line. To compensate the nonlinear characteristics of the control valve, linearized control input derived from the relation between control input and effective area of control valve and dither signal are used. The controller applied to the pneumatic driving apparatus is composed of the state feedback controller and the disturbance observer. The performance of the proposed method is evaluated by experiments and the experimental results show that position control error of 5 μm accuracy could be obtained easily by using the proposed method.

References

Hanafusa, H., 1982, "Design of Electrohydraulic Servo Control Systems for Articulated Robot Arm Control," *The Japan Hydraulics & Pneumatics Society*, Vol. 20, No. 7, pp. 429～436.

Helduser, S. and Muth, A., 1996, "Dynamic Friction Measurement Method Evaluated by Means of Cylinders and Valves," *Proceedings of the Third JHPS International Symposium on Fluid Power*, pp. 271～276.

Jang, J. S., 2002, "Position Control of a Pneumatic Cylinder with a Nonlinear Compensator and a Disturbance Observer," *Transactions of the KSME, A*, Vol. 25, No. 9, pp. 1795～1805.

Johira, T., 1997, "Pneumatic Servo System," *Transactions of the Japan Hydraulics and Pneumatics Society*, Vol. 28, No. 7, pp. 748～752.

Kawai, S., Kawakami, Y. and Masuda., 1993, "Some Consideration on the Position Control of Pneumatic Cylinder," *Proceedings of the Second JHPS International Symposium on Fluid Power*, pp. 563～568.

Kawashima, K., Oogami, H. and Yang, W. J., 1998, "Precision Intra-Stroke Stopping with a Precision of submicron in Pneumatic Cylinder," *Transactions of the Japan Hydraulics and Pneumatics Society*, Vol. 29, No. 4, pp. 95～99.

Kimura, T., Fujioka, H., Tokai, K. and Takamori, T., 2004, "Sampled-Data H_∞ Control for a Pneumatic Cylinder System," *Transaction of the Japan Fluid Power System Society*, Vol. 34, No. 3, pp. 62～65.

Kosaki, T. and Sano, M., 2002, "Computation of Friction Force in a Labyrinth-Sealed Pneumatic Cylinder," *Transactions of the Japan Hydraulics and Pneumatics Society*, Vol. 33, No. 1, pp. 9～14.

Lai, J. Y., Menq, C. H. and Singh, R., 1990, "Accurate Position Control of a Pneumatic Actuator," *Journal of Dynamic Systems, Measurement and Control*, Vol. 112, pp. 734～739.

McGuirk, D. P., Pingdong, W. and Xiao, X., 1998, "Fluid Power in the world," *Journal of the Japan Fluid Power System Society*, Vol. 29, No. 3, pp. 212～243.

Saito, T., Ikeda, H., Sugimoto, H. and Ikebe, J., 1995, "A Study on the Low Velocity Control of A Pneumatic Cylinder," *Journal of the Japan Hydraulics and Pneumatics Society*, Vol. 26, No. 6, pp. 804～810.

Situm, Z., Pavkovic, D. and Novakkovic, B., 2004, "Servo Pneumatic Position Control Using Fuzzy PID Gain Scheduling," *Journal of Dynamic Systems, Measurement and Control*, Vol. 126, pp. 376～387.

Tokashiki, L. R., Fujita, T., Kagawa, T. and Ikegami, T., 2000, "Stick-Slip Motion in Pneumatic Cylinder Driven by Meter Out Circuit," *Transactions of the Japan Fluid Power System Society*, Vol. 31, No. 6, pp. 170～175.

Yoshimitu, T. and Oyama, O., 2002, "Discrimination and Control of a Pneumatic Cylinder under Stick or Slip Mode of Seal," *Transactions of the Japan Fluid Power System Society*, Vol. 33, No. 3, pp. 57～62.